Wind and Structures, *Vol. 24, No. 4 (2017) 351-365*
DOI: https://doi.org/10.12989/was.2017.24.4.351

Alternative numerical method for identification of flutter on free vibration

Nakhyun Chun[1a], Jiho Moon[2b] and Hak-Eun Lee[*1]

[1]*School of Civil, Environmental and Architectural Engineering, Korea University, Seoul 02841, Republic of Korea*
[2]*Department of Civil Engineering, Kangwon National University, Chuncheon-si, Gangwon-do 24341, Republic of Korea*

(Received October 12, 2016, Revised February 10, 2017, Accepted February 22, 2017)

Abstract. The minimization method is widely used to predict the dynamic characteristics of a system. Generally, data recorded by experiment (for example displacement) tends to contain noise, and the error in the properties of the system is proportional to the noise level (NL). In addition, the accuracy of the results depends on various factors such as the signal character, filtering method or cut off frequency. In particular, coupled terms in multimode systems show larger differences compared to the true value when measured in an environment with a high NL. The iterative least square (ILS) method was proposed to reduce these errors that occur under a high NL, and has been verified in previous research. However, the ILS method might be sensitive to the signal processing, including the determination of cutoff frequency. This paper focused on improving the accuracy of the ILS method, and proposed the modified ILS (MILS) method, which differs from the ILS method by the addition of a new calculation process based on correlation coefficients for each degree of freedom. Comparing the results of these systems with those of a numerical simulation revealed that both ILS and the proposed MILS method provided good prediction of the dynamic properties of the system under investigation (in this case, the damping ratio and damped frequency). Moreover, the proposed MILS method provided even better prediction results for the coupling terms of stiffness and damping coefficient matrix.

Keywords: system identification; flutter derivatives; free vibration

1. Introduction

Flutter is a phenomenon caused by the self-excitation of structures initially induced by wind. Because of this phenomenon, a bridge could collapse when a critical wind speed is reached (Simiu and Scalan 1996). Therefore, flutter derivatives must be determined to compute the exact onset velocity of flutter instability. The signal character, filtering method, cutoff frequency and system identification (SID) methods all influence the accuracy of flutter derivatives. In these systems, indirect flutter

*Corresponding author, Professor, E-mail: helee@korea.ac.kr
[a]Ph.D. candidate, E-mail: nhchun84@gmail.com
[b]Assistant Professor, E-mail: jmoon1979@kangwon.ac.kr

http://www.techno-press.com/journals/was&subpage=7 ISSN: 1226-6116 (Print), 1598-6225 (Online)

derivatives, which are coupled terms, are particularly sensitive to noise and tend to have a big difference between their estimated and true values (Chowdhury and Sarkar 2003).

The free vibration technique, forced vibration technique, and a combination of these techniques are used to extract flutter derivatives. The free vibration technique is easily applicable to this test (Chowdhury and Sarkar 2003). Because the position of the model can be determined freely by the interaction of the fluid and structure, the free vibration techniques can properly simulate actual conditions. However, compared to the other test methods, this method is relatively more affected by surrounding circumstances. The free vibration technique is affected adversely by high frequency components of flow separation, the nonlinearity of large spring displacements and noise from the measuring devices, as such errors accumulate for the data. The forced vibration technique is more complex and the interaction between fluid and structure is difficult to simulate because the model moves along a planned route (Fuyou *et al*. 2016). However, the results can be easily evaluated because they are mainly affected by only device related problems such as a finite sampling rate (Sarkar *et al.* 2009). The combined technique described by Hwang *et al*. (2014) showed that the interaction between fluid and structure was accurately implemented. The excited location is linked with a spring system, which has actual dynamic properties, and this is set to move simultaneously with the structures. However, this method needs to be further verified since only a small amount of data has been generated and analyzed.

The present study is based on the free vibration technique which can simulate the response of a structure under actual conditions. This study uses displacement information as the reference variable. To evaluate velocity and acceleration one should use a differencing method. Errors accumulate upon differentiation and all methods mentioned above need to deal with contaminated signals. Specifically, indirect flutter derivatives ($H_2^*, H_3^*, A_1^*, A_4^*$) are sensitive to the noise to signal ratio in two degrees of freedom (2DOF).

Research on the flutter phenomenon was initiated by Scalan and Tomko (1971). Since the extraction of flutter derivatives was difficult, methods to enhance extraction have been developed. Sarkar (1992) developed the modified Ibrahim time domain (MITD) method to extract all direct- and cross-flutter derivatives from the coupled free vibration data of a 2DOF section model. Sarkar *et al*. (1992) identified eight flutter derivatives simultaneously from noisy displacement time-histories generated under laminar and turbulent flow. Chen *et al*. (2002) developed SID methods by using the general least square (GLS) theory for extracting 18 flutter derivatives. A complicated step is required for this GLS method wherein the complex mode theory and the MITD method should be used to find the initial value. The MITD method depends on time shifts N1 and N2. In addition, the time shift variables must be determined for optimal performance. On the other hand, the proposed method used a simple initial value and was stabilized using the linear least-square (LS) method. Chowdhury and Sarkar (2003) developed a method to extract 18 flutter derivatives in 3DOF by using the ILS method. However, the LS for the sum of the power of all residuals should be minimized when considering the possibility of all events occurring together. Therefore, none of the flutter derivatives cannot change after the estimation procedure of the ILS method. The proposed method can improve the accuracy of flutter derivatives after applying the ILS method through the use of correlation coefficients. The proposed method was applied to various numerical models.

Flutter derivatives respond to the solution of the homogeneous problem because such problems contain stiffness and damping coefficients. The ILS method correctly predicts the damping ratio and natural frequency, which accurately evaluates the critical velocity. However, the ILS method is occasionally prone to compute inaccurate flutter derivatives. No other technique has been

developed to improve the accuracy of flutter derivatives after using the ILS algorithm. The global solution (the damping ratio and damped frequency) is sensitive to each component of the system matrix and thus the accuracy of flutter derivatives is important to obtain reasonable results. For example, a wrong onset velocity can be computed when one uses mixed flutter derivatives extracted by different methods.

The proposed method using a correlation coefficient was investigated through a series of numerical analyses. Hereinafter, the procedure to compute the damping ratio and damped frequency is referred to as global approach, and the method to adjust system matrix components after the ILS method is referred to as the local approach. The local approach can enhance the quality of the flutter derivatives under high NL conditions. Two numerical models were constructed and verified to evaluate the accuracy of the computed flutter derivatives. The numerical model described by Jakobsen and Hjorth-Hansen (1995) was verified for use as a reference model. Based on this verified reference model, a series of parametric studies were conducted to investigate the effect of noise, following which another model was verified under various NL conditions. All numerical verifications were conducted in 2DOF. Finally, methods to apply the proposed algorithm were introduced. The proposed method gave reasonable predictions of flutter derivatives without significant loss of accuracy.

2. Flutter analysis of free vibration technique

To extract flutter derivatives a sequence of initial system matrices were introduced. Since the residuals are included in each variable when computing the flutter derivatives, the equation of motion becomes nonlinear. For this reason, the GLS method described by Ghilani and Wolf (2006) was adopted for extraction of flutter derivatives with the free vibration technique.

2.1 Equation of motion

To describe windy condition, the general equation of motion is

$$\underline{\underline{M}} \cdot \underline{\ddot{X}} + \underline{\underline{C}} \cdot \underline{\dot{X}} + \underline{\underline{K}} \cdot \underline{X} = \underline{F}_{se} + \underline{F}_{ad} \tag{1}$$

where,

$$\underline{X} = \left[h \;\; \theta \;\; p\right]^T,\; \underline{\underline{M}} = \begin{bmatrix} m_h & 0 & 0 \\ 0 & I_\theta & 0 \\ 0 & 0 & m_p \end{bmatrix},\; \underline{\underline{C}} = \begin{bmatrix} C_{11} & C_{12} & C_{13} \\ C_{21} & C_{22} & C_{23} \\ C_{31} & C_{32} & C_{33} \end{bmatrix},\; \underline{\underline{K}} = \begin{bmatrix} K_{11} & K_{12} & K_{13} \\ K_{21} & K_{22} & K_{23} \\ K_{31} & K_{32} & K_{33} \end{bmatrix}$$

$$\underline{F}_{se} = \begin{bmatrix} 0.5\rho U^2 B & 0 & 0 \\ 0 & 0.5\rho U^2 B^2 & 0 \\ 0 & 0 & 0.5\rho U^2 B \end{bmatrix} \begin{bmatrix} \frac{KH_1^*}{U} & \frac{KH_2^* B}{U} & \frac{KH_5^*}{U} & \frac{K^2 H_4^*}{B} & K^2 H_3^* & \frac{K^2 H_6^*}{B} \\ \frac{KA_1^*}{U} & \frac{KA_2^* B}{U} & \frac{KA_5^*}{U} & \frac{K^2 A_4^*}{B} & K^2 A_3^* & \frac{K^2 A_6^*}{B} \\ \frac{KP_5^*}{U} & \frac{KP_2^* B}{U} & \frac{KP_1^*}{U} & \frac{K^2 P_6^*}{B} & K^2 P_3^* & \frac{K^2 P_4^*}{B} \end{bmatrix} \begin{bmatrix} \dot{h} \\ \dot{\theta} \\ \dot{p} \\ h \\ \theta \\ p \end{bmatrix}$$

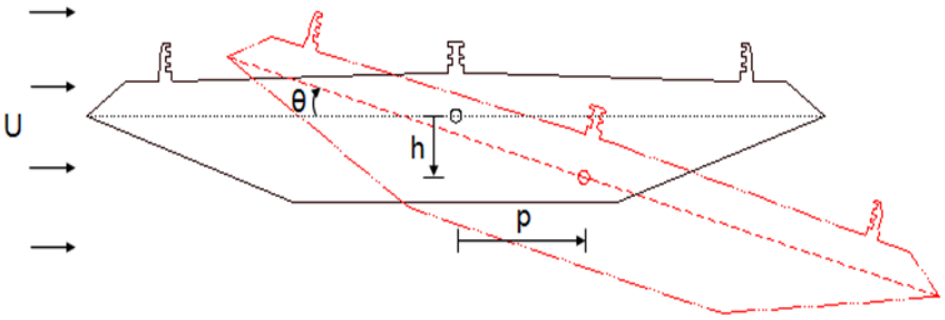

Fig. 1 Positive sign convention of 3DOF motion

F_{ad}: aerodynamic force by buffeting

Flutter analysis is conducted under uniform flow conditions, so the aerodynamic force is negligible. The self-excited force term can thus be moved to the left-hand side and the previous terms can be rewritten as

$$\underline{\underline{M}} \cdot \ddot{\underline{X}} + \underline{\underline{C}}^{eff} \cdot \dot{\underline{X}} + \underline{\underline{K}}^{eff} \cdot \underline{X} = 0 \tag{2}$$

Fig. 1 presents the general sign convention of dynamic response in wind engineering. Downward of vertical, rightward of lateral and clockwise of torsional displacement are positive at the mass center. Displacement is in units of meter and rotation is in units of radian when solving whole equations. The h, p and θ axes, shown in Fig. 1, are the global coordinates used in this study. Note that vertical and torsional sign convention is different from conventional structural analyses. Wind moving from left to right is denoted as positive.

2.2 Procedure for flutter analysis

2.2.1 State-space form

Dynamic equations are expressed in an effective form that can be organized into four differential equations. The state-space equation is

$$\begin{Bmatrix} \dot{X} \\ \ddot{X} \end{Bmatrix} = \begin{bmatrix} 0 & I \\ -M^{-1}K & -M^{-1}C \end{bmatrix} \begin{Bmatrix} X \\ \dot{X} \end{Bmatrix} \quad \text{or} \quad \dot{\underline{X}} = \underline{\underline{A}} \cdot \underline{X} \tag{3}$$

The iterative procedure to get matrix $\underline{\underline{A}}$ will be explained in section 3. The solution of the first order matrix differential equation is shown below

$$\underline{X} = e^{\underline{\underline{A}}t} \underline{X}^0 \tag{4}$$

where, $\underline{X}^0$ is the initial condition.

2.2.2 General least square (GLS) method

Xu *et al*. (2014) highlighted the possible causes for the nonlinearity of flutter derivatives. Because errors are difficult to quantify exactly, each output such as displacement, velocity and

acceleration must contain residuals at each point in time. Moreover residuals express possible cause for error as a single noise variable for each output. The equation of motion is assumed to contain residuals for each measurement, which is expressed by Eq. (5)

$$F(\underset{\sim}{X},\dot{\underset{\sim}{X}},\ddot{\underset{\sim}{X}}) = (\ddot{\underset{\sim}{X}} + \underset{\sim}{V}_{\ddot{X}}) + \underline{C}^{eff}(\dot{\underset{\sim}{X}} + \underset{\sim}{V}_{\dot{X}}) + \underline{K}^{eff}(\underset{\sim}{X} + \underset{\sim}{V}_{X}) \tag{5}$$

The Matrices C, K, and V_i presented in Eq. (5) are unknowns, and V_i, which is residual, is represented by $\ddot{h},\ \dot{h},\ h,\ \ddot{\theta},\ \dot{\theta},\ \theta,\ \ddot{p},\ \dot{p},\ p$. Because Eq. (5) involves a product of two unknowns, it is a nonlinear equation (Chun 2011)

$$\begin{aligned}
&(\ddot{h}+V_1)+C_{11}^{eff}(\dot{h}+V_2)+C_{12}^{eff}(\dot{\theta}+V_3)+C_{13}^{eff}(\dot{p}+V_4)+K_{11}^{eff}(h+V_5)+K_{12}^{eff}(\theta+V_6)+K_{13}^{eff}(p+V_7)=0\\
&(\ddot{\theta}+V_8)+C_{21}^{eff}(\dot{h}+V_9)+C_{22}^{eff}(\dot{\theta}+V_{10})+C_{23}^{eff}(\dot{p}+V_{11})+K_{21}^{eff}(h+V_{12})+K_{22}^{eff}(\theta+V_{13})+K_{23}^{eff}(p+V_{14})=0\\
&(\ddot{p}+V_{15})+C_{31}^{eff}(\dot{h}+V_{16})+C_{32}^{eff}(\dot{\theta}+V_{17})+C_{33}^{eff}(\dot{p}+V_{18})+K_{31}^{eff}(h+V_{19})+K_{32}^{eff}(\theta+V_{20})+K_{33}^{eff}(p+V_{21})=0
\end{aligned} \tag{6}$$

The Fourier expansion series can be adopted when solving this nonlinear equation

$$\begin{aligned}
&\frac{\partial F}{\partial \ddot{h}}V_{\ddot{h}}+\frac{\partial F}{\partial \dot{h}}V_{\dot{h}}+\frac{\partial F}{\partial h}V_h+\frac{\partial F}{\partial \dot{\alpha}}V_{\dot{\alpha}}+\frac{\partial F}{\partial \alpha}V_{\alpha}+\frac{\partial F}{\partial \dot{p}}V_{\dot{p}}+\frac{\partial F}{\partial p}V_p+\frac{\partial F}{\partial C_{11}^{eff}}dC_{11}^{eff}+\frac{\partial F}{\partial C_{12}^{eff}}dC_{12}^{eff}+\frac{\partial F}{\partial C_{13}^{eff}}dC_{13}^{eff}\\
&+\frac{\partial F}{\partial K_{11}^{eff}}dK_{11}^{eff}+\frac{\partial F}{\partial K_{12}^{eff}}dK_{12}^{eff}+\frac{\partial F}{\partial K_{13}^{eff}}dK_{13}^{eff}=\ddot{h}+C_{11}^{eff}\dot{h}+C_{12}^{eff}\dot{\alpha}+C_{13}^{eff}\dot{p}+K_{11}^{eff}h+K_{12}^{eff}\alpha+K_{13}^{eff}p\\
&\frac{\partial F}{\partial \ddot{\alpha}}V_{\ddot{\alpha}}+\frac{\partial F}{\partial \dot{h}}V_{\dot{h}}+\frac{\partial F}{\partial h}V_h+\frac{\partial F}{\partial \dot{\alpha}}V_{\dot{\alpha}}+\frac{\partial F}{\partial \alpha}V_{\alpha}+\frac{\partial F}{\partial \dot{p}}V_{\dot{p}}+\frac{\partial F}{\partial p}V_p+\frac{\partial F}{\partial C_{21}^{eff}}dC_{21}^{eff}+\frac{\partial F}{\partial C_{22}^{eff}}dC_{22}^{eff}+\frac{\partial F}{\partial C_{23}^{eff}}dC_{23}^{eff}\\
&+\frac{\partial F}{\partial K_{21}^{eff}}dK_{21}^{eff}+\frac{\partial F}{\partial K_{22}^{eff}}dK_{22}^{eff}+\frac{\partial F}{\partial K_{23}^{eff}}dK_{23}^{eff}=\ddot{\alpha}+C_{21}^{eff}\dot{h}+C_{22}^{eff}\dot{\alpha}+C_{23}^{eff}\dot{p}+K_{21}^{eff}h+K_{22}^{eff}\alpha+K_{23}^{eff}p\\
&\frac{\partial F}{\partial \ddot{p}}V_{\ddot{p}}+\frac{\partial F}{\partial \dot{h}}V_{\dot{h}}+\frac{\partial F}{\partial h}V_h+\frac{\partial F}{\partial \dot{\alpha}}V_{\dot{\alpha}}+\frac{\partial F}{\partial \alpha}V_{\alpha}+\frac{\partial F}{\partial \dot{p}}V_{\dot{p}}+\frac{\partial F}{\partial p}V_p+\frac{\partial F}{\partial C_{31}^{eff}}dC_{31}^{eff}+\frac{\partial F}{\partial C_{32}^{eff}}dC_{32}^{eff}+\frac{\partial F}{\partial C_{33}^{eff}}dC_{33}^{eff}\\
&+\frac{\partial F}{\partial K_{31}^{eff}}dK_{31}^{eff}+\frac{\partial F}{\partial K_{32}^{eff}}dK_{32}^{eff}+\frac{\partial F}{\partial K_{33}^{eff}}dK_{33}^{eff}=\ddot{p}+C_{31}^{eff}\dot{h}+C_{32}^{eff}\dot{\alpha}+C_{33}^{eff}\dot{p}+K_{31}^{eff}h+K_{32}^{eff}\alpha+K_{33}^{eff}p
\end{aligned} \tag{7}$$

We assumed that the residual is consistent over the entire process regardless of time and the discretized form of the equation. As such, it is constructed in matrix form as

$$\underline{B}\cdot\underline{V}+\underline{dA}\cdot\underline{J}=\underline{L} \tag{8}$$

The correction matrix can be computed as

$$\underline{dA}_{((2\times DOF)\times(2\times DOF))}=(\underline{L}_{((2\times DOF)\times N)}\cdot\underline{X}^{T}_{(N\times(2\times DOF))})(\underline{J}_{((2\times DOF)\times N)}\cdot\underline{X}^{T}_{(N\times(2\times DOF))})^{-1} \tag{9}$$

where N is the amount of data acquired over time. The final solution is the sum of the initial and correction matrix

$$\underline{A}=\underline{A}_0+\underline{dA} \tag{10}$$

where $\underline{A}$ is the effective stiffness and damping coefficient matrix and $\underline{J}$ is the Jacobian matrix

The general procedure for solving nonlinear equations of motion was introduced by using information above. The GLS method is used to solve the nonlinear equation. Because we deal with a nonlinear problem, the correction in matrix $\underline{A}$ is included in the initial approximation. The initial value is generally obtained by the LS method. The aim of these procedures is to extract the matrix $\underline{A}$, which consists of matrices $\underline{C}$ and $\underline{K}$. Matrix $\underline{A}$ represents mechanical damping when there is no wind. This study assumes that the weight matrix equals the identity matrix, which means that each variable has equal effect. The procedure to obtain the flutter derivatives is explained in section 3.

3. Proposed numerical process

Because displacement data is easily measured in the free vibration technique, the equation of motion is generally solved by variables that are discretized by displacement data. Errors accumulate during the differentiation process, and then, are sequentially applied during discretization. Therefore, the coupling terms can be affected severely by these errors in a multimode system. For example, H_2^*, H_3^*, A_1^*, and A_4^* are sensitive to the data quality under 2DOF. In this study, the central differencing method is used for discretization.

Because the filtering mainly influences the coupling term, this study suggests a method to change only the coupling term when finding the solution. For this reason, the choice of cutoff frequency is mentioned when using the filtering method. Additionally, the method that uses both the iterative general least square system identification procedure and the correlation coefficient approach is referred to hereafter as the MILS method. Details of the solution algorithm are given below.

3.1 Distortion of filtering

As signal filtering can remove unnecessary information in the frequency domain, it has a dramatic effect on noisy signals. However, signal filtering can easily distort signals in multimode systems, and thus, should be used with care. This study used a low-pass filtering method. The FIR filter was used to filter for consistency and the Kaiser window method was used in Matlab (James *et al*. 2003). A 200 Hz sampling rate was used in this study. The cutoff frequency factor is equal to multiply each eigen-frequency and factor. Fig. 2 presents the error in the results versus cutoff frequency factor. Each model is constructed with three types of NL. The NL described by Sarkar (1992) indicates, as a percentage, how many errors are contained in a signal, and is shown below

$$NL(\%) = \frac{\sqrt{E(\eta_i^2)}}{\sqrt{E(Y_i^2) - E(\eta_i^2)}} \times 100 \tag{11}$$

where Y_i, η_i are elements of the vectors $\underline{Y}, \underline{\eta}$, respectively, and $E(\cdot)$ denotes the expected value.

If the NL is high, the quality of the signal is poor. The black markers in Fig. 2 indicate a unity NL, red indicates an NL of 10, and green indicates a NL of 20. The X axes give the ratio of design frequency to the representative frequency of each DOF. The Y axes give the error in the form of the difference ratio between the true and simulated values of the system matrix components.

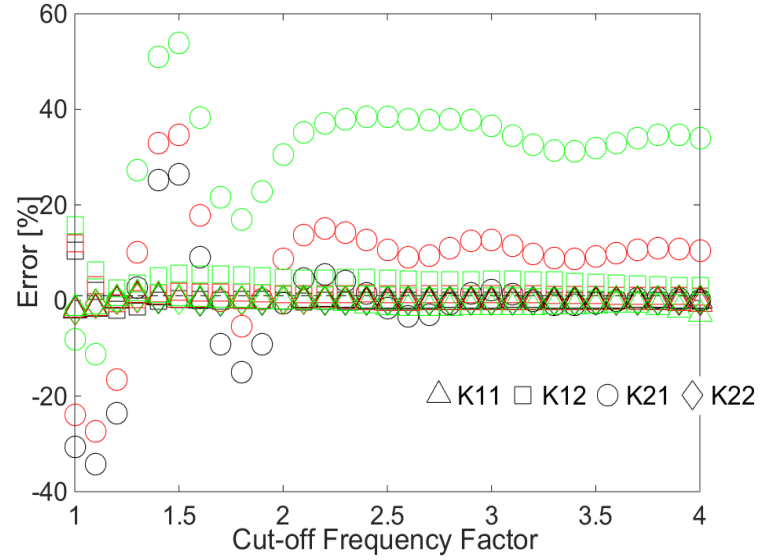

(a) Error for the stiffness

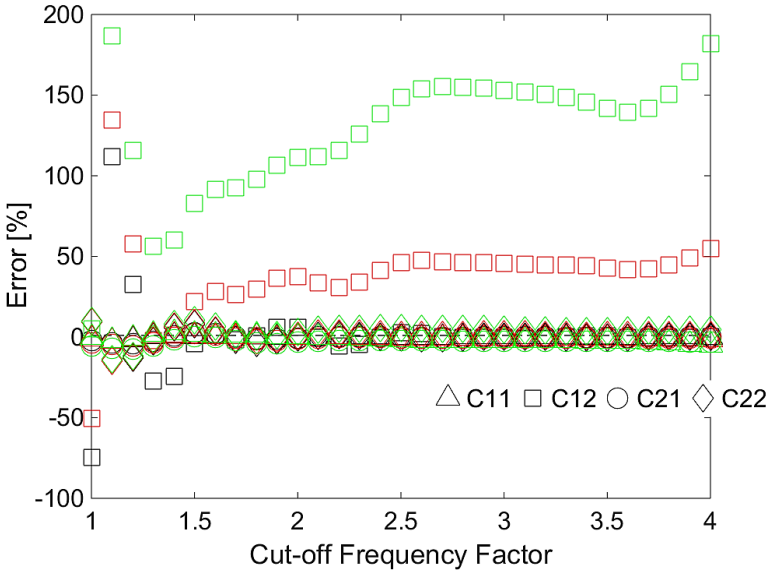

(b) Error for the damping coefficient

Fig. 2 Error of system matrix components as a function of cutoff frequency factor in model 1 (the cutoff frequency factor is equal to multiply each eigen-frequency and factor)

The cutoff frequency strongly influences the covariance terms in Fig 2. The error in the coupling terms is markedly different when the cutoff frequency factor is less than 1.5. In addition, a change of sign often seems to occur in a particular range of cutoff frequency. The stability of the solution is assured when the cutoff frequency factor exceeds two for vertical motion. If the ratio of torsional to vertical frequency exceeds two, a filtering method should be applied to the torsional data. In torsional motion, the solution is stable with a cutoff frequency of 1.3-2.2. For multimode

systems, the cutoff frequency factor of the lowest frequency should exceed the ratio of the highest frequency to lowest frequency. To solve our problems, we introduce in section 3.2 technique that involve the correlation scheme. Because it is significantly affected by cutoff frequency, only the covariance terms of the system matrix are adjusted according to step (8) in the section 3.2.

3.2 Algorithm of proposed method

Chowdhury and Sarkar (2003) proposed the ILS method, which matched properly with the numerical case. However, in some cases the results are inappropriate. Furthermore, if poor results are computed once in the ILS method, the problem cannot be fixed. For this reason, a new approach needs to be considered. Usually cross derivatives $(H_2^*, H_3^*, A_1^*, A_4^*)$ are sensitive to the NL in 2DOF, so the adjustment matrix that can handle the coupling term is introduced as step (8). Herein, to obtain better results, we introduce a new strategy that involves verification in 2DOF. The iterative general least square (IGLS) method is used from step (1) to (7) and is similar to the ILS method. The proposed algorithm is introduced in step (8).

(1) construct velocity and acceleration from filtered displacement X_0

(2) construct X that is a matrix of vertical and rotation motion that consist of displacement and velocity

(3) obtain matrix A_0 by using LS : $A_0 = (\dot{X}_0 X_0^T)(X_0 X_0^T)^{-1}$

(4) set $X_1 = e^{\left[A_0\right]t} X^0$, X^0 is the initial condition

(5) obtain matrix A_i by using GLS : $dA_i = (LX_i^T)(JX_i^T)^{-1}$, $A_i = A_{i-1} + dA_i$ $(i = 1, 2, \ldots, k)$

(6) set $X_i = e^{\left[A_{i-1}\right]t} X^0$, and then repeat steps (4)-(6)

(7) perform until $\max\left|A_i - A_{i-1}\right| < \textit{iteration level}$, and then, compute matrix A

(8) apply adjustment coefficients (a, b, c, d) to covariance terms in matrix A

$$\left[\tilde{A}_i\right] = \begin{bmatrix} 0 & 0 & 1 & 0 \\ 0 & 0 & 0 & 1 \\ -K_{11} & -a \cdot K_{12} & -C_{11} & -c \cdot C_{12} \\ -b \cdot K_{21} & -K_{22} & -d \cdot C_{21} & -C_{22} \end{bmatrix}, \text{ and then } \left[\tilde{A}_0\right] = [A]$$

(9) compute $\tilde{X}_i$ for a, b, c, d : $X_i = e^{\left[A_{i-1}\right]t} X^0$

(10) find maximum of correlation coefficient, not for velocity, but between the filtered displacement and approximated displacement : $C_i = \rho(X_0, \tilde{X}_i)$

(11) obtain several a, b, c, d that satisfy the condition $C_i > C_{i-1}$

(12) find maxima and minima of a, b, c, d , and then, these shall be the new bounds

(13) repeat (8)~(12) five times

(14) perform until $\max\left|C_i - C_{i-1}\right| < \textit{iteration level}$, and then compute matrix A, which must satisfy the convergence criteria

We now give a detailed explanation of the algorithm. The GLS method is similar to the ILS method shown in step (1) to (7) apart from the fact that the GLS method handles a nonlinear problem so the correction value is considered in step (5). In addition, the approximated value in step (9) is obtained using bounded values thorough step (8). Bounded values should be considered

Table 1 Numerical model

Model	K [N/m]		C [N·s /m]		ω_h [*Hz*] / ω_θ [*Hz*]	Ratio of frequency	ζ_h[%] / ζ_θ[%]
Model 1	420.100	-59.181	8.931	-0.080	2.016	2.546	0.156
			0.435	0.039	5.133		0.023
Model 2	1.755	19.659	0.040	-0.080	2.016	2.543	0.024
			0.435	0.039	5.127		0.023

carefully: if the range of bounds is too broad, calculation times become unmanageably long. In contrast, if the range of bounds is too narrow, the appropriate solutions cannot be computed. This study uses bounded values from -1.5 to 1.5 and the initial step size of 0.3 for each adjustment coefficient. The updated bounded value from step (12) is newly defined and classified into a certain ratio in step (8), as follows

$$n_i = \frac{\Delta\varphi_i}{\sum_{k=1}^{DOF^2} \Delta\varphi_k} n_t \tag{12}$$

Here the index i denotes each adjustment coefficient, $\Delta\varphi_i$ presents the step size that is the difference between the largest and smallest adjustment coefficient, n_i presents the number of steps for each adjustment coefficient and n_i presents the total number of steps, which is $10\times DOF^2$. Previous maxima and minima are turned into the newly bounded values in step (12). Each DOF has correlation coefficient values for use in step (10). At this point, the order in which the correlation values are applied is important. The procedure in step (10) and (11) consists of five steps. It is performed three times for the adjusted coefficient of the DOF that has the largest correlation value, whereas the unsatisfied coefficient is excluded through step (11). The same procedure is applied twice for the remaining adjusted coefficient of the other DOF that has lower correlation. For 3DOF, we repeat this process three times for the adjusted coefficient of the DOF that has the largest correlation, while the unsatisfied coefficient is excluded through step (11). The same procedure is repeated twice for the remaining adjusted coefficient of the DOF that has the middle correlation value, while the unsatisfied coefficient is excluded through step (11). The same procedure is then repeated twice for the remaining adjusted coefficient of the DOF that has the lowest correlation value. Because displacement data is precise when using the free vibration technique, the proposed algorithm focuses on displacement data. As a result, the procedure that deals with correlation coefficients between the measured and approximated displacement signal is vital for success. The method to apply this correlation scheme can make corrections in the time domain and enhance the damping ratio and damped frequency.

4. Numerical case study

4.1 Description of numerical case

The proposed method, which is MILS, using the above procedure was used to a find solutions for numerical models. The simulations performed with two models, which were implemented in 2DOF. The first model described by Jakobsen and Hjorth-Hansen (1995) is used as reference model and the second model was constructed by modifying the damping coefficient matrix of the first model. Because accurate damping ratios are difficult to estimate in dynamic systems, only the damping coefficient matrix is modified from the original signal shown in Table 1. To analyze the effect of noise, each model was tested under three cases that consist of NL of 1, 10, and 20. Figures in Table 1 are the true values. The values that are estimated by the MILS method are all simulated values and are compared with the true values.

In model 1 (2), the vertical damping ratio is 0.1559% (0.236%) and the torsional damping is 0.0226% (0.0227%). Each damping ratio was evaluated from a non-proportional damping analysis. In model 1 (2), the vertical damped frequency is 2.0157 Hz (2.0157 Hz) and the torsional damped frequency is 5.1325 Hz (5.1268 Hz). The mass is 2.6526 and the mass moment of inertia is 0.0189. The stiffness and damping coefficients follow the MKS unit. All values in Table 1 were rounded to three decimal places.

4.2 Results of numerical case

Tables 2-5 show the differences between the true and simulated values. The subindices of K and C denotes rows and columns, respectively. Tables 2 and 3 present results obtained using the ILS method. The damping ratio and damped frequency are almost same as the true values. In other words, the ILS method appropriately predicts the on-set velocity for flutter. For example, if the damping ratio or damped frequency is negative, the bridge has reached collapse. However, each component of the system matrix is sensitive to the NL. Note that the procedure to obtain the final solution by using the LS method, such as for the damping ratio or frequency, can be considered a global approach and the process to find each component of the matrix can be considered a local approach. The LS method can find a very accurate final solution since it is satisfied when the possibility of all events occurring together is the highest. However, if each component of the matrix is evaluated with erroneous value, there are limitations in correcting it. On the contrary, the MILS method can handle local problems by adopting adjustment coefficients locally, instead of just considering the global problem, because it includes the LS method

Table 2 Error in accuracy for the ILS method (model 1)

NL	K12 (%)	K21 (%)	C12 (%)	C21 (%)	ζ_h(%)	ζ_θ(%)
1	-9.515	7.065	-6.506	0.136	-1.924	2.212
10	-6.044	19.151	51.576	-2.502	-1.219	1.327
20	-2.081	49.420	118.027	-4.952	-0.513	4.867

Table 3 Error in accuracy for the ILS method (model 2)

NL	K12 (%)	K21 (%)	C12 (%)	C21 (%)	ζ_h(%)	ζ_θ(%)
1	0.622	-1.588	38.994	0.302	1.271	-2.203
10	-5.770	5.128	37.922	0.460	-4.661	-2.203
20	-2.189	-0.225	-433.252	5.185	1.271	-1.322

Table 4 Error in accuracy for the MILS method (model 1)

NL	K12 (%)	K21 (%)	C12 (%)	C21 (%)	ζ_h(%)	ζ_θ(%)
1	-0.467	12.418	-15.856	0.136	-0.706	-1.327
10	-4.721	6.109	19.771	-0.288	-0.641	0.000
20	7.883	21.363	-55.398	5.785	2.502	-3.097

Table 5 Error in accuracy for the MILS method (model 2)

NL	K12 (%)	K21 (%)	C12 (%)	C21 (%)	ζ_h(%)	ζ_θ(%)
1	0.622	3.333	205.787	0.302	2.119	-2.643
10	-5.770	-0.655	-17.272	0.460	-5.085	-2.203
20	-2.638	8.654	-62.281	1.058	-1.271	-0.441

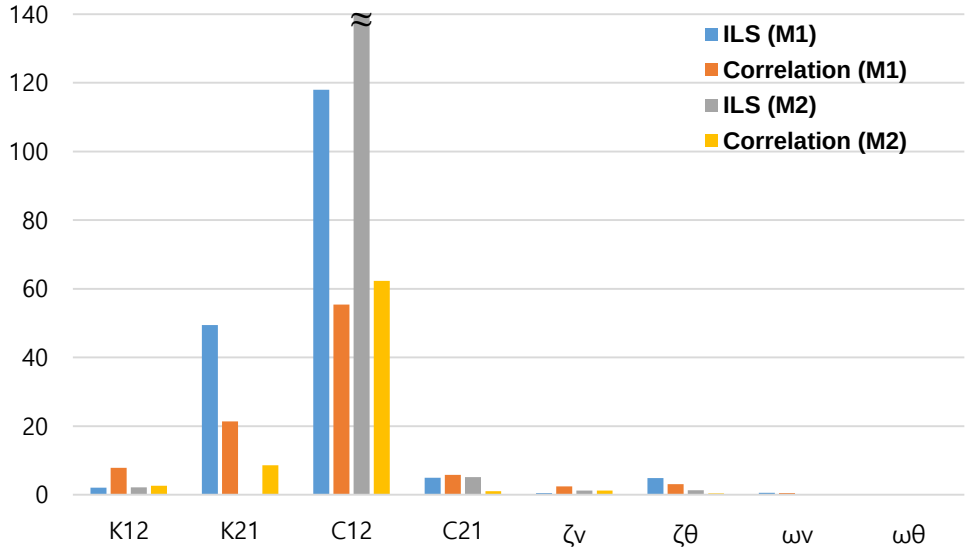

Fig. 3 Comparison between the ILS and MILS methods

For the ILS method, the damping ratio is accurate regardless of the NL, but the coupling term of each component is sensitive to the NL. Tables 4 and 5 present results of local problems that are improved when the correlation method is used to solve these problems.

The error of covariance term is reduced in Tables 4 and 5. Specifically, the stiffness term corresponds better to the true values. Because the diagonal term is fixed, these results are reliable when the filtering process is performed appropriately. Fig. 3 presents a summary of the test results. The ILS method is limited in terms of its local approach, but the MILS method works well when using a local approach. However, distorted results can be obtained with the proposed method when the NL is low. For a low NL, the signal itself is so clear that the global approach is better for computing the true value. When using the MILS method for a low NL, the signals have multiple correlations coefficients with high accuracy. In addition, the correlations of the approximated signal are higher than those between the true value and measured signal. For this reason, some components of the system matrix are computed poorly in the MILS method. In other words, one

needs to determine whether the correlation method should be applied. This can be determined from specific correlation values. The correlation coefficient is conservatively determined to exceed 0.9995 for an almost true signal. Consequently, it is suggested that 0.9995 be used as the reference value when using the MILS method; that is, only if the correlation coefficient is less than 0.9995 should the MILS method be used.

Fig. 3 presents the errors of the whole model under NL 20 (M1 and M2 denotes models 1 and 2, respectively). Both methods have high accuracy for the global solution. The highest error in the global solution is the torsional damping ratio, at 4.87%, in the ILS method. The errors of K21 and C12 are relatively large among the coupling terms. The MILS method performs accurately except for K21 of model 2. Overall, the proposed method shows good results for these two models. Upon solving the complex eigenvalue problems of the non-proportional damping system, the true system has a vertical damping of 0.1559 and torsional damping of 0.0226 in model 1. In the ILS method, we obtain a vertical damping of 0.1551 and a torsional damping of 0.0237. In the proposed method, the vertical damping is 0.1598 and torsional damping is 0.0219. Additionally, the true system has a vertical damping of 0.0236 and torsional damping of 0.0227 in model 2. In the ILS method, a vertical damping is 0.0239 and torsional damping is 0.0224 in model 2. In the proposed method, the vertical damping is 0.0233 and torsional damping is 0.0226. Moreover, for the ILS method in model 1, the approximated values of K12, K21, C12, and C21 are -57.9487, 2.6226, -0.1742 and 0.4130, respectively. For the proposed method in model 1, the approximated values of K12, K21, C12, and C21 are -63.8457, 2.1302, -0.0356 and 0.4596, respectively. In the ILS method in model 2, approximated values of K12, K21, C12, and C21 are -57.8850, 1.7512, 0.266269 and 0.4570, respectively. For the proposed method in model 2, approximated values of K12, K21, C12, and C21 are -57.6193, 1.9071, -0.0301 and 0.4391, respectively. All values in Tables 2-5 are rounded to three decimal places.

The simulation, which uses the numerical results of model 1, is compared with the true values in the time domain. Fig. 4 is based on model 1 from Jakobsen and Hjorth-Hansen (1995), the green line represents the true values and the blue line shows the filtered signal. The simulation agrees well with the true values for vertical and rotational values.

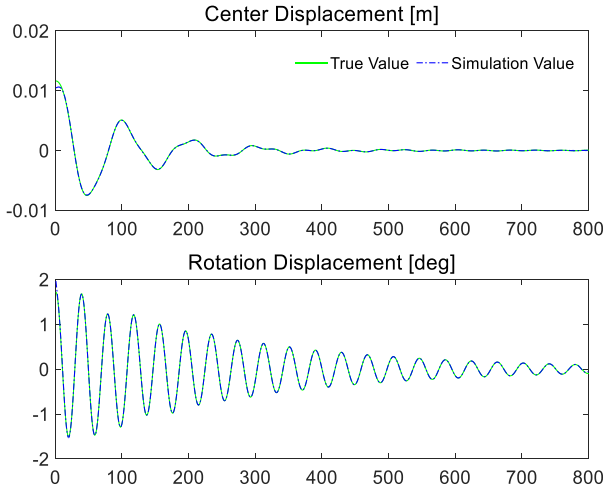

Fig. 4 Time history results with high vertical damping and low torsional damping

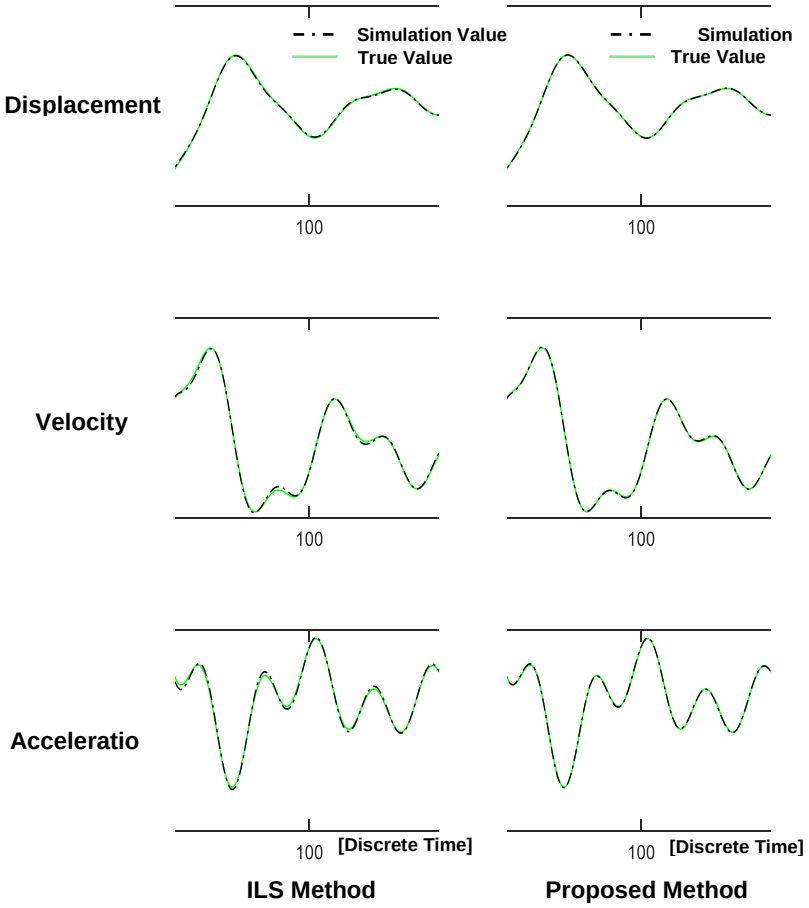

Fig. 5 Comparison between the ILS and proposed method

Fig. 5 presents detailed results of the MILS method. Displacement, velocity, and acceleration are well matched by using the correlation scheme and are superior to the results obtained with the ILS method when NL is 20. Both methods accurately reflect the tendencies of the true values; however, the results are not accurate in a certain range when magnifying the graph of displacement, velocity and acceleration. However, compared to the ILS method, the proposed method provides results that better match with the true values.

To summarize, the global approach clearly presents the tendency of the signal, whereas the local approach produces greater accuracy and reflects the actual tendency. Our results show that the MILS method is more effective for a higher NL.

5. Conclusions

This paper introduced the MILS method, which was based on displacement data. The ILS method is a global approach that focuses on a systemic problem. Consequently, the ILS method is difficult to enhance local problems, while the proposed scheme can be applied to local problems.

In other words, the MILS method uses both global and local approaches, and thus can be considered as a new SID method. To obtain better performance, more models that have high non-proportionality must be verified and the adjustment of diagonal terms needs to be considered regardless of filtering in further works.

The cutoff filtering factor cause the results of the coupling term to be biased, so the cutoff frequency should be carefully determined before applying the proposed method. In multimode systems, the lowest cutoff frequency factor must be higher than the ratio of highest to lowest frequency.

The accuracy of the results depended on the level of the NL. Specifically, the MILS method performed well in high NL, while for low NL, the ILS method generally delivered more accurate results than the MILS method because the multiple optimal correlation values between the simulated and measured signals were higher than the correlation between the true and measured signals. For this reason, the ILS method is suitable when correlation coefficient exceeds 0.9995, whereas the MILS method is proper in other cases.

References

Chen, A., He, X. and Xiang, H. (2002), "Identification of 18 flutter derivatives of bridge decks", *J. Wind Eng. Ind. Aerod.*, **90**(12), 2007-2022.

Chowdhury, A.G. and Sarkar, P.P. (2003), "A new technique for identification of eighteen flutter derivatives using a three-degree-of-freedom section model", *Eng. Struct.*, **25**(14), 1763-1772.

Chun, N.H. (2011), "System identification of flutter derivatives extraction with independent variables", M.S. Dissertation, Korea University, Seoul.

Fuyou, X., Xuyong, Y. and Zhe, Z. (2016), "Insight into coupled forced vibration method to identify bridge flutter derivatives", *Wind Struct.*, **22**(3), 273-290.

Ghilani, C.D. and Wolf, P.R. (2006), *Adjustment Computations: Spatial Data Analysis*, John Wiley and Sons, Inc, Hoboken, New Jersey, USA.

Hwang, Y.C., Kim, H.K., Cha, S.H. and Lee, H.S. (2014), "New excitation technique for the identification of flutter derivatives", *Proceedings of the 2014 World Congress on Advances in Civil, Environmental, and Materials Research*, Busan, August.

Jakobsen, J.B. and Hjorth-Hansen, E. (1995), "Determination of the aerodynamic derivatives by a system identification method", *J. Wind Eng. Ind. Aerod.*, **57**, 295-305.

James, H.M., Ronald, W.S. and Mark, A.Y. (2003), *Signal Processing First*, Prentice Hall, Upper Saddle River, New Jersey, USA.

Sarkar, P.P. (1992), "New-identification methods applied to the response of flexible bridges to wind", Ph.D. Dissertation, MD: The Johns Hopkins University, Baltimore.

Sarkar, P.P., Caracoglia, L., Haan, Jr. F.L., Sato, H. and Murakoshi, J. (2009), "Comparative and sensitivity study of flutter derivatives of selected bridge deck sections, Part 1: Analysis of inter-laboratory experimental data", *Eng. Struct.*, **31**(1), 158-169.

Sarkar, P.P., Jones, N.P. and Scanlan, R.H. (1992), "System identification for estimation of flutter derivatives", *J. Wind Eng. Ind. Aerod.*, **41-44**, 1243-1254.

Scanlan, R.H. and Tomko, J.J. (1971), "Airfoil and bridge deck flutter derivatives", *J. Eng. Mech. Div.*, ASCE, **97**(6), 1717-1733.

Simiu, E. and Scalan, R.H. (1996), *Wind Effects on Structures*, John Wiley and Sons, Inc., Hoboken, New Jersey, USA.

Xu, F., Zhu, L., Ge, X. and Zhang, Z. (2014), "Some new insights into the identification of bridge deck flutter derivatives", *Eng. Struct.*, **75**, 418-428.

CC